

Impulsive phase flare energy transport by large-scale Alfvén waves and the electron acceleration problem

L. Fletcher¹

lyndsay@astro.gla.ac.uk

Department of Physics and Astronomy, University of Glasgow, Glasgow G12 8QQ

H. S. Hudson

hhudson@ssl.berkeley.edu

Space Sciences Laboratory, University of California, Berkeley, CA 94720

ABSTRACT

The impulsive phase of a solar flare marks the epoch of rapid conversion of energy stored in the pre-flare coronal magnetic field. Hard X-ray observations imply that a substantial fraction of flare energy released during the impulsive phase is converted to the kinetic energy of mildly relativistic electrons (10-100 keV). The liberation of the magnetic free energy can occur as the coronal magnetic field reconfigures and relaxes following reconnection. We investigate a scenario in which products of the reconfiguration – large-scale Alfvén wave pulses – transport the energy and magnetic-field changes rapidly through the corona to the lower atmosphere. This offers two possibilities for electron acceleration. Firstly, in a coronal plasma with $\beta < m_e/m_p$, the waves propagate as inertial Alfvén waves. In the presence of strong spatial gradients, these generate field-aligned electric fields that can accelerate electrons to energies on the order of 10 keV and above, including by repeated interactions between electrons and wavefronts. Secondly, when they reflect and mode-convert in the chromosphere, a cascade to high wavenumbers may develop. This will also accelerate electrons by turbulence, in a medium with a locally high electron number density. This concept, which bridges MHD-based and particle-based views of a flare, provides an interpretation of the recently-observed rapid variations of the line-of-sight component of the photospheric magnetic field across the flare impulsive phase, and offers solutions to some perplexing flare problems, such as the flare “number problem” of

¹Carried out while a Visiting Researcher, Space Sciences Laboratory, University of California, Berkeley, CA

finding and resupplying sufficient electrons to explain the impulsive-phase hard X-ray emission.

Subject headings: Sun:flares,corona; waves; acceleration of particles

1. Introduction

Strong chromospheric hard X-ray emission and strong UV and white-light emission mark the impulsive phase of a solar flare. These signatures are usually interpreted in terms of the well-known “thick-target model” (Brown 1971; Hudson 1972) in which fast electrons lose energy in Coulomb collisions and ionizing collisions in the chromosphere, heating and producing bremsstrahlung *en route*. The inefficiency of the bremsstrahlung process in a cold thick target implies that a large fraction of flare energy resides in these electrons (Kane & Donnelly 1971; Lin & Hudson 1976; Holman et al. 2003), and calculations under the assumptions of the thick-target model yield numbers on the order of $10^{34} - 10^{37}$ electrons accelerated per second (e.g. Miller 1997; Holman et al. 2003). Various strands of evidence have led to the commonly-accepted idea that the particle acceleration takes place in the solar corona, following which the electrons propagate into the lower atmosphere where they heat, and generate the observed hard X-ray radiation. Extensive theoretical work over four decades (which we will not attempt to summarize here) has elucidated the basics and the specifics of numerous different coronal acceleration mechanisms, in the electric fields present in current-sheets and X-lines/points generated by reconnection, in large- and small-scale plasma waves and turbulence, and at shocks. Recent reviews can be found in Aschwanden (2002) or Litvinenko (2003), for example. However, a coronal acceleration site still presents some problems for theory. The primary difficulty, especially in the context of the high intensity of the energy deposition implied not only by hard X-rays but also by UV and white-light continuum observations (e.g. Fletcher et al. 2007), is the so-called “number problem” - the high total number of electrons required compared to that available in the corona - and the associated (and in fact more problematical) supply and re-supply problems.

The thick-target model as normally understood requires intense electron beams to transport the flare energy. We propose instead that flare energy is transported by the Poynting flux of Alfvén waves. Since flare energy release implies large-scale restructuring of the coronal magnetic field (e.g. via reconnection) it is natural to expect the excitation of such waves (Emslie & Sturrock 1982). The electron acceleration can then take place where the waves dissipate, in the legs of the coronal loops or in the chromosphere itself.

The possibility of flare energy transport by Alfvén waves has been discussed before,

for example by Emslie & Sturrock (1982) in the context of heating the temperature minimum region, and more generally by Melrose (1992) and Wheatland & Melrose (1994) who examined the propagation of twist in a flare loop. The present paper seeks to restart the discussion of flare wave energy transport, in the light of recent solar observations and recent developments in magnetospheric physics, as well as because of the outstanding theoretical issues with coronal electron acceleration, which have been exacerbated by RHESSI, TRACE and other observations.

The main solar physics drivers for revisiting this idea are as follows. Firstly, recent microwave (gyrosynchrotron) observations of the corona above active regions demonstrate conclusively that magnetic field strengths of several hundredths up to more than a tenth of a Tesla (i.e. several 100s of Gauss to kG) exist in the cores of active regions, measured at heights up to 10,000 - 15,000 km above the photosphere. Coupled with reasonable coronal densities of 10^{15}m^{-3} these fields imply Alfvén wave speeds well above 10^4 km s^{-1} , and correspondingly high Poynting fluxes. The observational basis for these physical parameters described in some detail in Section 2.3. Secondly, there is clear evidence that substantial perturbations to the photospheric magnetic field (on the order of 0.01 to 0.02 T) occur during solar flares. Field changes in the low corona, on height scales comparable to the horizontal dimensions of active regions, must be of similar magnitude. This strongly suggests a violent perturbation to the magnetic field, at a low level in the atmosphere, which is at least qualitatively consistent with a very energetic magnetic disturbance

In magnetospheric physics, electron acceleration in the parallel electric field that results from the propagation of large-scale Alfvén waves and wave pulses in a non-idealised MHD fluid is a promising prospect for auroral electron acceleration, and also motivates us in this work. In the magnetospheric/ionospheric context it was pointed out early on that non-ideal effects arise from considering both the two-fluid nature of the plasma (i.e. treating electrons as a separate fluid, and including their inertia and thermal pressure) and also the particle aspects of the problem (e.g., the finite ion gyroradius). These lead to field-aligned electric fields, and the presence of such dispersive Alfvén waves and their link to electron acceleration is now well-established observationally (e.g. Wygant et al. 2002). Chaston et al. (2002) have demonstrated that the value of the energy flux carried by auroral electrons is similar to the Poynting flux of low frequency Alfvén oscillations of the magnetospheric field. Debates persist about the precise mechanism for generating the electric fields that accelerate auroral electrons (e.g., Stasiewicz et al. 2000), but the inertial Alfvén wave (see Section 3.1) is a strong candidate. This may also have a role to play in the case of flares, although the solar and magnetospheric cases of course represent very different parameter regimes. We demonstrate in Section 3.1 that the inertial Alfvén wave mode is also the appropriate one to consider for flare parameters. The critical factor in determining the parallel electric field

that can be generated is the spatial scale of perpendicular structuring of the magnetic field compared to the electron inertial length, and - as we describe - observations at ever higher resolution are showing finer and finer magnetic field structuring.

We note also that electron acceleration by non-ideal MHD waves is also making its way into the discussion of coronal heating. Stasiewicz (2006) and Stasiewicz et al. (2007) claim that dispersive Alfvén waves driven by photospheric turbulence lead to parallel electric fields and electron heating, and Tsiklauri (2006) finds the generation of a parallel electric field and runaway electron heating when an initially ideal (non-dispersive) but non-linear Alfvén wave couples to dissipative modes when it is launched into a corona with transverse density structure. Our considerations are somewhat different from this idea, in that our inertial Alfvén wave is dispersive from the start. This does not preclude also the kind of mode coupling discussed by Tsiklauri (2006); instead this would be an additional energy loss term which will require further study in the future.

We first describe the proposed mechanism in Section 2, including a detailed description of the observations that motivate us. The hard X-ray observations, as confirmed by RHESSI, require powerful electron acceleration, and in Section 3 we discuss possibilities for this in the framework of the wave transport model. Section 4 then considers the overall implications for flare energetics.

2. The proposed mechanism

2.1. The waves

2.1.1. Wave source

The release of stored magnetic energy requires a re-structuring of the field, for example as envisioned in large-scale magnetic reconnection. However the amount of magnetic free energy that can be *dissipated* within the reconnection region itself – current sheet, X-point or 3-D null – is restricted, given its small dimensions and the short flare time-scale. The more important release of free energy occurs in the large-scale ‘convulsion’ as the newly-reconnected magnetic field relaxes from its pre-flare stressed state. Where they detach from the coronal current-sheet or null structure but are still stressed, these magnetic field lines will be highly distorted from a potential configuration, with a locally high tension force. We know observationally that the impulsive energy release occurs in a highly-stressed magnetic field, with large fluctuations on time scales ranging down to a fraction of a second (e.g., Dennis 1985). This implies irregular and time-varying structures in a three-dimensional

reconnection flow. Thus Petschek reconnection, which is essentially steady-state, cannot properly describe it.

The rapid restructuring of the field implies an energy flow describable in terms of MHD wave propagation, and we infer that it will create a complicated mixture of fast-mode, slow-mode, and Alfvén-mode propagating wave pulses in the adjacent plasma. For example, flare loop ‘shrinkage’ (e.g., Forbes & Acton 1996) identifiable with the MHD fast mode is a simple and well-known illustration of this idea, as are the slow-mode shocks of Petschek fast reconnection. MHD modeling of three-dimensional reconnection is at an early stage, but in three dimensions a torsional component will in general also exist, particularly in a reconnecting twisted field (Emslie & Sturrock 1982). Indeed, in-situ observations of reconnection in the solar wind (Gosling et al. 2005) show Alfvén waves propagating along just-reconnected field lines, and the MHD simulations of Linton & Longcope (2006) demonstrate a post-reconnection state of initially untwisted flux tubes in which field-line kinks propagate away at close to the Alfvén speed. Since we require to deposit flare energy in the flare footpoints, we require a wave mode that propagates along the magnetic field - either the Alfvén mode or the slow mode. However, the slow mode speed is too low to explain the observed footpoint simultaneity unless we have extremely symmetric propagation from exactly half way between the footpoints. For the same reason of low speed, neither can it explain the require high energy flux (see Section 4). Thus, we work under the assumption of an Alfvénic disturbance carrying energy along the post-reconnection field.

2.1.2. *Wave development*

We sketch our overall view of a post-reconnection loop and the processes taking place in it in Figure 1. The perturbation in 3D takes the form of fast-mode and Alfvén-mode wave pulses (Emslie & Sturrock 1982); the group velocity of the Alfvén mode is parallel to the magnetic field \mathbf{B} , so this component of the energy propagates directly to the footpoints as shown in the cartoon. In the MHD view the propagation speed is just the Alfvén speed (in a kinetic treatment Goertz & Boswell 1979, also recovered this result).

The wave spectrum will be determined by the largely-unknown geometry of the energy release. It is likely that the Alfvén wave will take the form of a short-wavelength propagating pulse - a wavefront - with parallel wavelength much smaller than the length L of a just-reconnected loop. The perpendicular wavelengths would be much smaller than the loop length, as dictated by the reconnection rate and its fluctuations.

Under appropriate conditions (Section 2.3) the Alfvénic perturbation will propagate

rapidly through the coronal field to the chromosphere without significantly cascading to smaller scales. This is different from (but complementary to) the view of Larosa et al. (1994) and Miller (1997), in which the large-scale fast-mode waves formed by reconnection are assumed to cascade rapidly to short-wavelength turbulence within the coronal loop, leading eventually to the Fermi acceleration of electrons in high-frequency turbulence directly in the corona. For the ducted Alfvén mode it has been shown (e.g. Kinney & McWilliams 1998; Cranmer & van Ballegooijen 2005) that a cascade will not develop immediately. Therefore in the situation we envisage, the Alfvénic perturbation will move from corona to chromosphere along a strong guide field without driving a cascade, at least in the initial pass. The wave energy will be strongly ducted towards the chromosphere.

If some fraction of the wave energy is reflected at the chromosphere, so that counter-moving waves are present in the corona, then a cascade may occur. However, even then, Kinney & McWilliams (1998) demonstrate using reduced MHD simulations that the cascade to high parallel wavenumbers is inhibited, and an exponentially-decaying rather than a power-law spectrum will be formed, while the cascade to high *perpendicular* wave numbers proceeds independently.

On arriving at the chromosphere and photosphere the wave propagation will become more complicated, with transmission, reflection and damping all playing a role. The waves will undergo different kinds of damping, including – in the temperature-minimum region – significant ion-neutral damping. The line-tied boundary conditions at the photosphere mean that the purely Alfvén disturbance will not survive as such but instead, as demonstrated by Goedbloed & Halberstadt (1994), a reflected wave spectrum with hybrid characteristics will be generated, and some fast-mode-like components will arise, particularly in the presence of chromospheric small-scale structuring and flows. Being compressional, these fast-mode-like waves can be locally damped by other mechanisms, and offer also the possibility for a turbulent cascade development in the chromosphere, analogous to that proposed by Larosa et al. (1994) for coronal acceleration. The analysis of Goedbloed & Halberstadt (1994) suggested that any reflected waves that do re-emerge into the corona would have a mostly torsional (Alfvénic) character.

2.2. The particles

The hard X-ray observations unambiguously require powerful electron acceleration. How can this arise from energy transported in the Poynting flux of Alfvén waves? We discuss possible mechanisms in Section 3 and briefly comment here on the particle behavior in the context of Figure 1. In the new scenario the acceleration of the energetically important

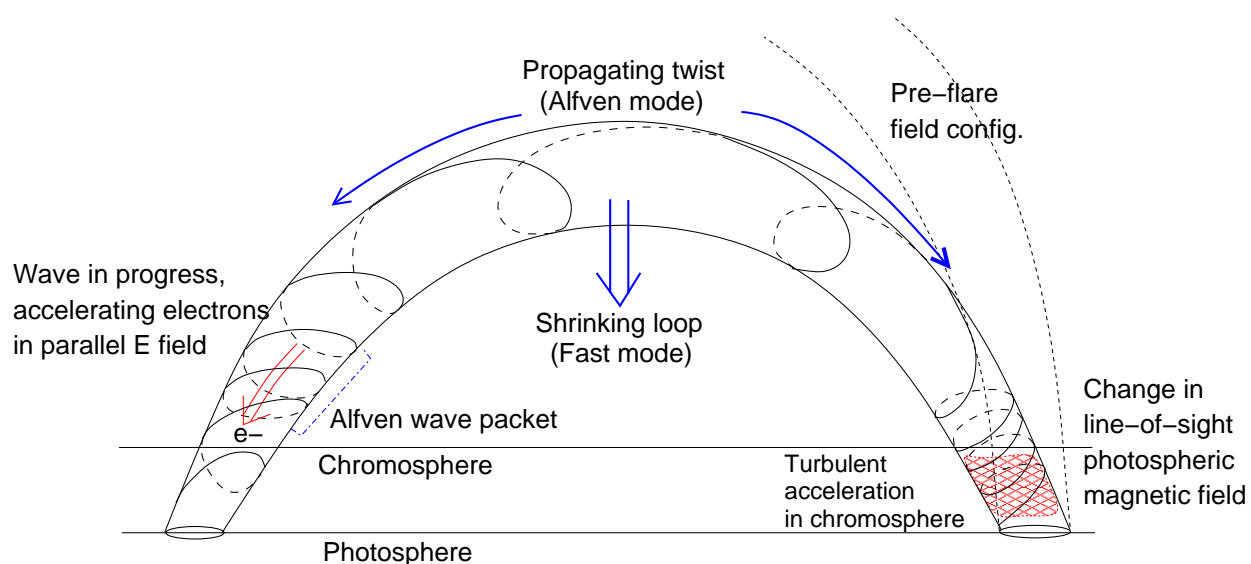


Fig. 1.— The reconfiguring coronal field launches a torsional Alfvén wave pulse through the corona and into the chromosphere, as well as a fast-mode wave pulse. The Alfvén wave, which propagates in the inertial regime, can lead to electron acceleration in the corona. That fraction of the Alfvén wave energy that survives into the chromosphere can also lead to stochastic acceleration there. The wave will be partially reflected from the steep gradients in the chromosphere (not shown) and re-enter the corona.

10-100 keV electrons either takes place in the legs of the flaring loops, or actually in their footpoint regions.

Alfvénic perturbations propagating in the limit $\beta < m_e/m_p$ (the inertial Alfvén wave limit) lead to a parallel electric field E_{\parallel} . For a wave traveling downwards, electron inertia produces an upwards E_{\parallel} . A fraction of the electrons are resonantly accelerated in this field, in a process that can be thought of as an encounter with a moving mirror (Kletzing 1994; Chaston 2006), with the electrons reflecting from the traveling perturbation front and accelerating to twice the Alfvén speed v_A . In the conditions we envisage, where the Alfvén speed is on the order of 0.1-0.3 c (see Section 2.3), this corresponds to an ‘Alfvén energy’ ($= \frac{1}{2}m_e v_A^2$) in the few to tens of keV range. Multiple reflections of the electron between the wave front and magnetic mirror formed by the converging chromospheric magnetic field may occur, each reflection from the wave front increasing the electron speed by $2v_A$ in first-order Fermi acceleration.

As mentioned in Section 2.1.2 a turbulent wave spectrum may be generated in the footpoint regions. In the chromosphere, the damping of this spectrum will broadly-speaking result in plasma heating, since the electron-electron thermalization times are very short. However, an essentially collisionless tail of fast electrons can be accelerated by Fermi processes, as in the case of coronal stochastic acceleration. The question is how large that tail may be. We discuss this in Section 3.4 but note here that stochastic acceleration can take place in a collisional environment (e.g., Hamilton & Petrosian 1992). The particular advantages offered by chromospheric acceleration are firstly a high ambient electron density (compared to the corona), possibly easing the number and resupply problems, and secondly - as pointed out by Brown (2006, private communication) and MacKinnon (2006) - , the requirement on the total number of accelerated electrons implied by their hard X-ray signature is reduced if the accelerator acts on them at the same time as they radiate bremsstrahlung emission, which would be satisfied in a chromospheric accelerator. (This advantage is analogous to the increased bremsstrahlung efficiency that pertains in a thermal model for flare hard X-rays, where the radiating electrons are continually re-boostered by interactions with a hot rather than a cold target (e.g. Smith & Lilliequist 1979).)

This overall scenario also provides a mechanisms for some accelerated electrons to appear in the corona. This is important because of the extensive observational evidence for coronal non-thermal electrons, e.g. via the microwave spectrum, or low energy hard X-rays. Any reflected component of the inertial Alfvén wave pulse produces a reversed electric field, which can draw chromospheric electrons back into the corona. Furthermore, coronal electron acceleration by the cascade of fast-mode turbulence - as proposed by Larosa et al. (1994) - may operate alongside the Alfvénic transport, as both wave types will be generated by the

reconnection process.

2.3. Physical Parameters

The properties of the Alfvén waves, and the magnitude of the parallel electric fields they generate, depend critically on the plasma parameters; density, electron and ion temperatures, magnetic field strength and length scales. We review the relevant observations here.

Magnetic field strength:

It is notoriously difficult to determine the strength of the coronal magnetic field, or to calculate it by extrapolations from a given boundary. However, in solar flares and in the cores of active regions, where the magnetic field is strong, simple geometrical arguments point to intense fields in the low corona. A large sunspot may have a size scale of some 3×10^4 km, an umbral field of a few $\times 0.1$ T, and an outer penumbral field of 0.08 to 0.17 T (Solanki 2003). For the dominant dipole term of a multipole expansion of this photospheric source structure, we would expect comparable coronal field intensities, at heights in the vicinity of the spot comparable to the spot extent.

Direct measurement of the strength of (strong) coronal magnetic fields is also possible via the microwave gyrosynchrotron spectrum generated by fast electrons. Very Large Array radio observations of active regions show emission consistent with *average* active region coronal field strengths of a few $\times 0.01$ T (Lee et al. 1998) at a height of 10,000 km above the photosphere. In the corona above sunspots, even stronger fields have been measured (White et al. 1991; Shibasaki et al. 1994; Brosius et al. 2002; Vourlidas et al. 2006; Brosius & White 2006). For example, using VLA and SOHO data, Brosius et al. (2002) deduce field strengths in excess of 0.1 T at heights of 10,000 km above the photosphere over a sunspot on the disk, and for a substantial area around it. Limb observations, with less confusion in the dependence of the field strength on altitude (Brosius & White 2006), also give these values. Based upon these observations, we can reasonably expect field strengths of a few $\times 0.01$ T at heights of 10,000 km above sunspot or strong plage regions, and since flare ribbons also penetrate into sunspot umbrae, low-coronal fields > 0.1 T are certainly not out of the question. These magnetic field strengths are substantially higher than the values inferred from coronal seismology, however the coronal seismology technique has only been applied so far to large active-region loops (e.g., Nakariakov & Ofman 2001).

The height of 10,000 km at which these strong fields are observed is also consistent with the height of loops involved in flares, based on their typical HXR footpoint separa-

tions of typically a few tens of arcseconds. There are not to our knowledge any statistical studies of this, but numerous examples can be seen in e.g. Sakao (1994), Bogachev et al. (2005), Battaglia & Benz (2006), Fletcher et al. (2007). A typical separation value of $30''$ or 20,000 km corresponds to a semicircular loop with apex height of 10,000 km.

Density: With the exception of coronal soft X-ray ‘knots’ (e.g. Doschek et al. 1995) and rare observations of dense coronal loop flares which show negligible footpoint emission (e.g. Veronig & Brown 2004), the coronal density before and early in a flare is fairly low. Several studies have sought pre-flare signatures of the bright flare loops but the general result is that in most cases no feature visible in soft X-rays matches the flare loops that form after the impulsive phase (Fárník et al. 1996; Fárník & Savy 1998). This suggests that the energy release takes place in regions of yet lower density than the average active-region corona. Normal active-region loop densities are on the order of $1 - 3 \times 10^{15} \text{cm}^{-3}$ (Del Zanna & Mason 2003) and even post-flare arcade loop measurements (Varady et al. 2000; Landi et al. 2003) are a few $\times 10^{15} \text{m}^{-3}$, which might reasonably be taken as an upper limit for the pre-flare density in the flare region. In the study of a sunspot magnetic field mentioned above, Brosius et al. (2002) estimated plasma densities at a few $\times 10^{14} \text{m}^{-3}$ to 10^{15}m^{-3} in the essentially ‘empty’ corona above a sunspot. Finally, Fletcher & De Pontieu (1999) find upper-transition region densities of $2 - 5 \times 10^{15} \text{m}^{-3}$ in the cores of active regions, again implying a lower density for the overlying hotter corona. Taken together, these various strands of evidence imply that pre-flare coronal densities on the order of 10^{15}m^{-3} or possibly smaller are common, and in many cases we have only upper limits.

Alfvén speed: If we take a magnetic field strength of 0.05 T and a proton number density $n_p = 10^{15} \text{m}^{-3}$, in a fully-ionized hydrogen plasma the Alfvén speed is $3.5 \times 10^4 \text{km s}^{-1}$. Higher values of $|\mathbf{B}|$ or lower values of n_p are also possible, so v_A could thus be a few $\times 0.1 c$. These may seem like extreme values given that the ‘canonical’ coronal value often discussed is on the order of 10^3km s^{-1} , and that fast coronal mass ejections – presumably ejected at some fraction of the local Alfvén speed – travel at around $3,000 \text{km s}^{-1}$ above a couple of solar radii. However the measurements, and our considerations, refer to the low corona, where the bulk of the magnetic energy resides, in highly-stressed, compact fields. Note that since $(v_A/c)^2 \ll 1$ the wave can still be described non-relativistically, and the displacement current may still be neglected, allowing an MHD description.

Assuming a loop half-length of 10^7m , the propagation time of such a wave into the chromosphere from a coronal launch site is a few tenths of a second at most. This is shown in Figure 2 for a hydrostatic corona at $T = 10^6 \text{K}$ matched to the top of the of the VAL-C chromospheric model (Vernazza et al. 1981), and using the chromospheric magnetic scaling

of Zweibel & Haber (1983), i.e., $|\mathbf{B}| \propto P_g^\alpha$, where P_g is the gas pressure. The parameter α has been chosen to give a field strength at the photosphere of 0.2 T. The propagation time obtained is adequate to explain the observed timescales of hard X-ray emission as well as the simultaneity of hard X-ray footpoints (Sakao 1994), an argument often advanced in favor of energy transport by energetic electrons accelerated in the corona and precipitating at the footpoints. The commonly-observed pattern of slower non-thermal variations in the later phase of a solar flare may result from the increase of coronal densities and decrease in the strength of the reconnecting fields in this phase, and thus reduced Alfvén speeds.

Photospheric magnetic perturbations: The observations of non-reversible changes to the line-of-sight magnetic field at the photospheric level mentioned in Section 1 lend credence to our supposition that strong perturbations to the magnetic field are present throughout the atmosphere. For example Cameron & Sammis (1999) and Kosovichev & Zharkova (2001) observed such changes in ground-based and SOHO/MDI data respectively. Sudol & Harvey (2005), using simultaneous SOHO/MDI and GONG magnetogram data, observe permanent line-of-sight photospheric magnetic changes (0.01-0.02 T) to be “ubiquitous features” of X-class flares at least. The changes are observed to be roughly co-spatial with the flare ribbons and occur rapidly, on timescales of minutes. They are therefore too fast to be due to Alfvénic perturbations propagating upwards from the sub-photospheric region. Rather, it is as if the magnetic field at the photospheric level is ‘jerked’ by the overlying magnetic field as it restructures in the corona, with both a twisting component and a loop retraction. The fact that we see a distortion to the photospheric magnetic field indicates that there is substantial wave energy transmitted to low levels in the atmosphere, although with present line-of-sight observations we cannot distinguish between components corresponding to twisting and retracting.

Transverse magnetic structuring: As will become apparent in Section 2.4, the transverse scale of magnetic structure is a vital parameter in our calculations, but observations are strongly limited by instrumentation. We do have observed upper limits to the transverse structuring of the chromospheric magnetic field in the quiet sun: in recent observations using the Swedish Vacuum Solar Telescope, Berger et al. (2004) report that magnetic elements seen in the G-band (the photosphere) appear unresolved at 70 km spatial resolution. We may expect that transverse photospheric structuring on still smaller scales may be present. A lower limit to the transverse scales would be the ion inertial length, in the range 10^{-2} –1 km at the transition region interface.

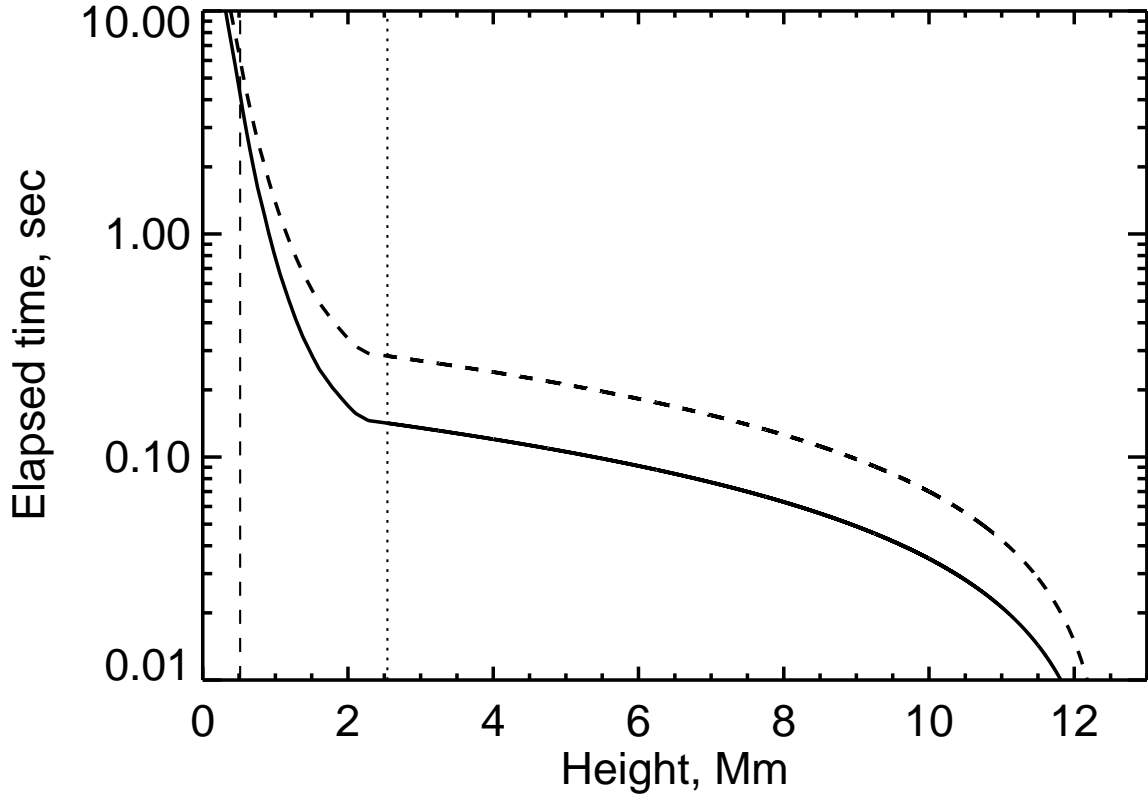


Fig. 2.— Propagation time at the Alfvén speed from loop top to a given height. The vertical dashed line indicates the temperature minimum, and the vertical dotted the top, of the VAL-C atmospheric model. This model is extended into the corona with a semicircular loop of coronal half-length 10,000 km and a density scale height given by the temperature assumed for the base of the corona, 10^6 K. The dashed curve shows a coronal field of 0.05 T, extended through the atmosphere with $\alpha = 0.052$ (see text); the solid curve the more extreme case of 0.1 T with $\alpha = 0.0$.

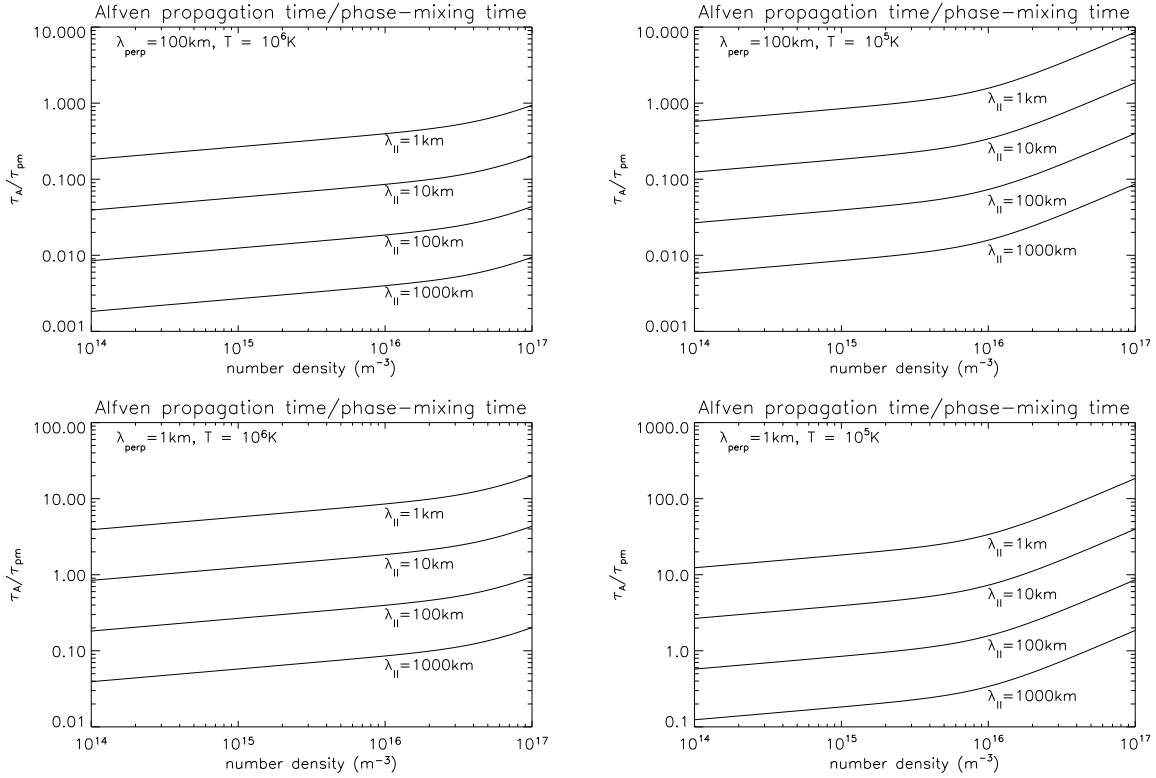


Fig. 3.— The ratio of the Alfvén propagation time along a 10^4 km loop to the damping time by phase mixing, for a different wavelength perturbations in a coronal field of $0.05 T$, a temperature of 10^6 K (left hand panel) and 10^5 K (right hand panel). The perpendicular wavelength of the perturbation is 10^2 km (upper row) and 1 km (lower row).

2.4. Wave passage through the corona

We establish here that the coronal Alfvén wave pulses can traverse the corona and arrive at the chromosphere without significant viscous or resistive damping. In a corona with strong non-uniformities perpendicular to the field, the damping of Alfvén waves is by phase mixing (e.g., Roberts 2000). The damping time is given by his Equation 22, expressed here in terms of the wavelength:

$$\tau_{pm} = \left(\frac{6\lambda_{\parallel}^2\lambda_{\perp}^2}{4\nu\pi^2v_a^2} \right)^{1/3} \quad (1)$$

where λ_{\parallel} and λ_{\perp} are the parallel and perpendicular wavelengths respectively. Under most conditions the viscosity ν is the plasma shear viscosity, ν_s , which is the kinematic viscosity multiplied by $(\omega_i\tau_i)^{-2}$ (Heyvaerts & Priest 1983) where ω_i is the ion gyrofrequency and τ_i the ion collision time. In circumstances where this factor is much less than unity, Joule dissipation will dominate, and the viscosity will be given by the magnetic diffusivity,

$$\nu_m = \frac{1}{(\mu_o\sigma)}, \quad (2)$$

with σ the Spitzer conductivity. The total viscosity we use in Eq. 1 is the sum of the shear and the Joule viscosity. Figure 3 compares the phase-mixing time scale to the Alfvén propagation time τ_A along the coronal part of the loop, This shows that $\tau_A/\tau_{pm} < 1$ for perturbations with parallel wavelengths of more than a few tens of km propagating in a coronal density of $\sim 10^{15}\text{m}^{-3}$. However, wave energy may be lost in accelerating particles, as we describe in the next section.

3. Electron acceleration in the context of energy transport by Alfvén wave pulses

If the wave energy is transported by ducted Alfvén wave pulses as we suggest, there are several possibilities for electron acceleration; we consider three, most closely related to the wave nature of the transport mechanism. Firstly, in a hot, tenuous, strongly magnetized coronal plasma, it may be possible to accelerate electrons directly in the corona, in the parallel electric field generated by a dispersive Alfvén wave pulse (Sections 3.1 and 3.2). Secondly, associated with this is the possibility that the electrons, accelerated ahead of the wavefront, mirror in the converging solar magnetic field and return for repeated interactions with the wave (Section 3.3). This comprises a first-order Fermi acceleration process. Thirdly, the wave energy can be dissipated in or near the chromosphere in a turbulent cascade which accelerates electrons stochastically (Section 3.4) and we discuss separately the two primary

models for turbulent electron acceleration; stochastic resonant acceleration in high frequency whistler turbulence, and transit-time acceleration in lower-frequency MHD turbulence. We consider first the acceleration by inertial Alfvén waves.

3.1. Inertial Alfvén waves

In ideal MHD, the (massless) negative charge carriers respond instantaneously to any parallel electric field generated by the Alfvénic perturbation, shorting it out so that no E_{\parallel} exists. An ideal MHD wave includes an E_{\perp} , but this does not accelerate particles. However, in a real plasma, the electrons have (i) a finite mass and therefore inertia, and (ii) a finite thermal speed and therefore a pressure. Both of these properties make parallel electric fields possible, which lead to the dissipation of the wave energy by electron energization. The importance of electron inertia in generating parallel electric fields in the magnetosphere/ionosphere was first discussed by Goertz & Boswell (1979).

We follow here the definitions of Stasiewicz et al. (2000), who give an overview of dispersive Alfvén waves. An inertial Alfvén wave (IAW) results if the electron thermal speed is smaller than or comparable to the Alfvén speed. The electric field is due to the finite inertia of the electrons, which cannot respond instantaneously to the wave perturbation. (If the electron thermal speed exceeds the Alfvén speed, but the electron pressure gradient is important, then wave is termed a kinetic Alfvén wave, or KAW). Alternatively, the conditions correspond to an IAW if $\beta \leq m_e/m_p$ (and a KAW if $m_e/m_p \leq \beta \leq 1$).

The plasma β is:

$$\beta = \frac{2\mu(n_p + n_h)k_B T \mu_o}{|\mathbf{B}|^2} \quad (3)$$

where k_B is Boltzmann’s constant, μ_o the permeability of the vacuum, T is the temperature (we assume that the electron and ion temperatures are equal), μ the mean molecular weight, n_p the proton number density and n_h the neutral hydrogen number density. Although the neutral hydrogen does not respond directly to the Alfvénic disturbance, it is strongly collisionally coupled to the ion component (e.g. De Pontieu et al. 2001) and thus modifies the Alfvén speed in the lower atmosphere. It also provides a mechanism for damping the wave in the lower atmosphere, which will locally heat the chromospheric plasma. Taking a mean molecular weight of 0.6, and assuming a completely ionized target of density $n_e = n_{15} \times 10^{15} \text{m}^{-3}$ and temperature $T = T_6 \times 10^6$ K, we have

$$\beta = \frac{2 \times 10^{-8} n_{15} T_6}{|\mathbf{B}|^2}, \quad (4)$$

for $|\mathbf{B}|$ in T. So, for example, if $|\mathbf{B}| = 0.05$, $n_{15} = 1$, $T_6 = 1$, $\beta = 8 \times 10^{-6}$, and the waves are inertial. The inertial regime pertains for substantial distances into the chromosphere (down to about 1500 km above the photosphere in the VAL-C semi-empirical model). Note that in other regions of the solar atmosphere, such as in long active region loops with a relatively small magnetic field, the KAW is appropriate, but not in the high magnetic field strength relevant to a flare.

We have in mind an IAW disturbance with the form of a wave pulse or simple wave, a case considered by Kletzing (1994) and Watt & Rankin (2007). However, acceleration in IAWs is also discussed in the context of global resonances of the magnetospheric field (e.g., Wright et al. 2002; Wright & Hood 2003; Wright et al. 2003), which could be established by repeated partial reflections of the IAW from the photospheric or low chromospheric boundary. Evidently, the exact nature of the oscillation will have to be determined in a self-consistent way along with the particle acceleration.

3.2. The electric field strength and electron energy

Described in two-fluid MHD, a large-scale Alfvénic perturbation causes particle cross-field drifts; an $\mathbf{E} \times \mathbf{B}$ drift equal for both species, and a polarization drift. The ion polarization drift is a factor m_i/m_e faster than that of the electrons, constituting a net cross-field current, the magnitude of which depends on the wave amplitude at a given position. A field-aligned current of electrons flows to maintain plasma quasi-neutrality.

From Stasiewicz et al. (2000), their Equation 47, the relationship between the perpendicular electric field E_\perp and the change in the perpendicular magnetic field b_\perp is

$$E_\perp = v_A b_\perp (1 + k_\perp^2 \lambda_e^2)^{1/2}, \quad (5)$$

which is a modification of the ideal MHD relationship. Here $k_\perp = 2\pi/\lambda_\perp$ is the perpendicular wavenumber of the magnetic disturbance and λ_e is the electron skin depth ($= c/\omega_{pe}$; ω_{pe} being the electron plasma frequency). In Eq. 5 we have also used the fact that the perpendicular scale of the magnetic disturbance is much larger than the ion Larmor radius (see also Chaston et al. 2002).

The relationship between the parallel and perpendicular components of the wave is given by Stasiewicz et al. (2000), Equation 43:

$$E_\parallel = \left(\frac{k_\parallel k_\perp \lambda_e^2}{1 + k_\perp^2 \lambda_e^2} \right) E_\perp \quad (6)$$

where k_\parallel is the parallel wavenumber. While in the magnetosphere, the ratio $k_\perp^2 \lambda_e^2$ can be

comparable to unity, in the solar atmosphere it is typically much less than unity. Therefore the ratio between parallel and perpendicular electric field in the solar atmosphere is going to be small in the solar atmosphere. However, since the perpendicular electric field calculated from Eq. 5 is large, this small fraction can still result in a parallel field large enough to be interesting. In the absence of precise knowledge about these scales we investigate the parameter regimes in which substantial field-aligned electric fields might be obtained.

To be effective in accelerating electrons, E_{\parallel} must exceed the local Dreicer field, E_D (Dreicer 1959; Spicer 1982), above which the bulk of the thermal electron distribution will be freely accelerated (‘runaway’). The Dreicer field, E_D , is

$$E_D = \frac{e \ln \Lambda}{4\pi\epsilon_o\lambda_D^2} = \frac{e \ln \Lambda}{4\pi\epsilon_o^2} \frac{ne^2}{\epsilon_o k_B T}, \quad (7)$$

where $\ln \Lambda$ is the Coulomb logarithm, ϵ_o the permittivity of free space and λ_D is the Debye length. $\ln \Lambda$ is usually taken to be between 20 and 25 for the corona. In the partially ionized plasma of the lower chromosphere, $\ln \Lambda$ is modified to $x \ln \Lambda + (1 - x) \ln \Lambda'$ where x is the ionization fraction and $\ln \Lambda'$ the ‘effective Coulomb logarithm’ describing the interaction of charged and neutral particles (see e.g., Brown 1973).

Neglecting the temperature-dependence of the Coulomb logarithm, the ratio of the parallel electric field to the Dreicer field in the corona is

$$\frac{E_{\parallel}}{E_D} = 10^5 \frac{T_6}{n_{15}^{5/2}} \frac{|\mathbf{B}| b_{\perp}}{l_{\parallel} l_{\perp}} \quad (8)$$

where l_{\parallel} , l_{\perp} the parallel and perpendicular wavelengths in kilometers and $|\mathbf{B}|$, b_{\perp} are in T. Evidently, only in hot, tenuous, strongly-magnetized plasmas will this ratio exceed unity; the ratio is plotted in Figures 4 and 5, where it can be seen that at a coronal density of 10^{15}m^{-3} , $\frac{E_{\parallel}}{E_D}$ exceeds unity only for scales $l_{\parallel} \sim 10 - 100 \text{ km}$ and $l_{\perp} \leq 5 \text{ km}$. Increasing the temperature, field strength, or the perturbation amplitude, or decreasing the length-scale of the perturbation gives a higher value for $\frac{E_{\parallel}}{E_D}$. However, wave-generated super-Dreicer fields are not possible in the chromosphere for realistic parameters of the ambient medium or perturbation.

A full calculation of the electron energy spectrum accelerated must be left for future investigations, as it requires a simulation capable of following the non-linear evolution of the wave and of the electron distribution function (e.g., Watt et al. 2004; Damiano & Wright 2005). But we can observe that, in a corona of density $5 \times 10^{14} \text{m}^{-3}$, super-Dreicer fields are produced in strong fields, by propagating wave pulses having parallel wavelengths of around 100 km and perpendicular wavelengths of around 5 km. Electrons with a thermal speed similar to the wave phase speed can be accelerated, via a single interaction with the

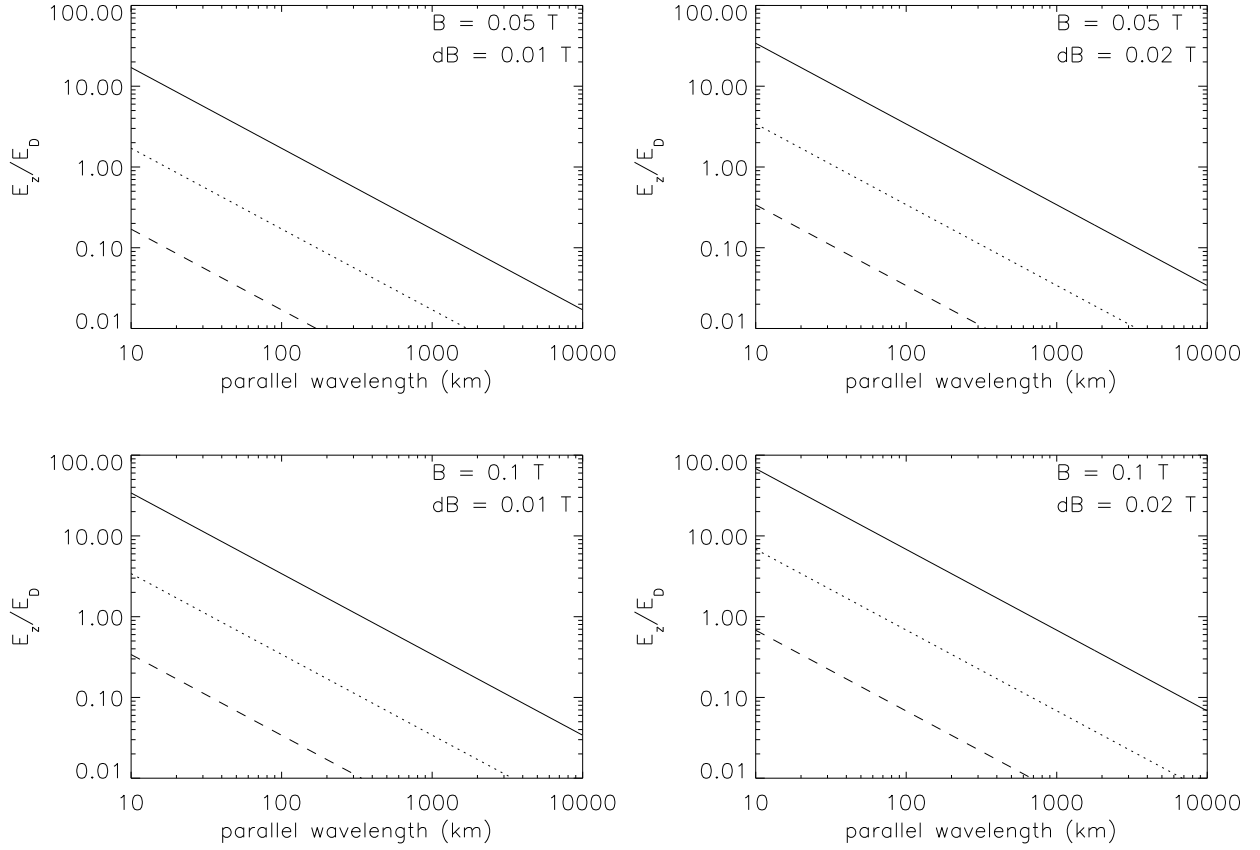


Fig. 4.— The ratio of parallel electric field to Dreicer field for field and perturbation values given in the top right corner of each panel. The local coronal electron density is 10^{15}m^{-3} and the temperature is 10^6 K. The lines correspond to $\lambda_{\perp}=0.5$ km (solid), 5 km (dotted), 50 km (dashed).

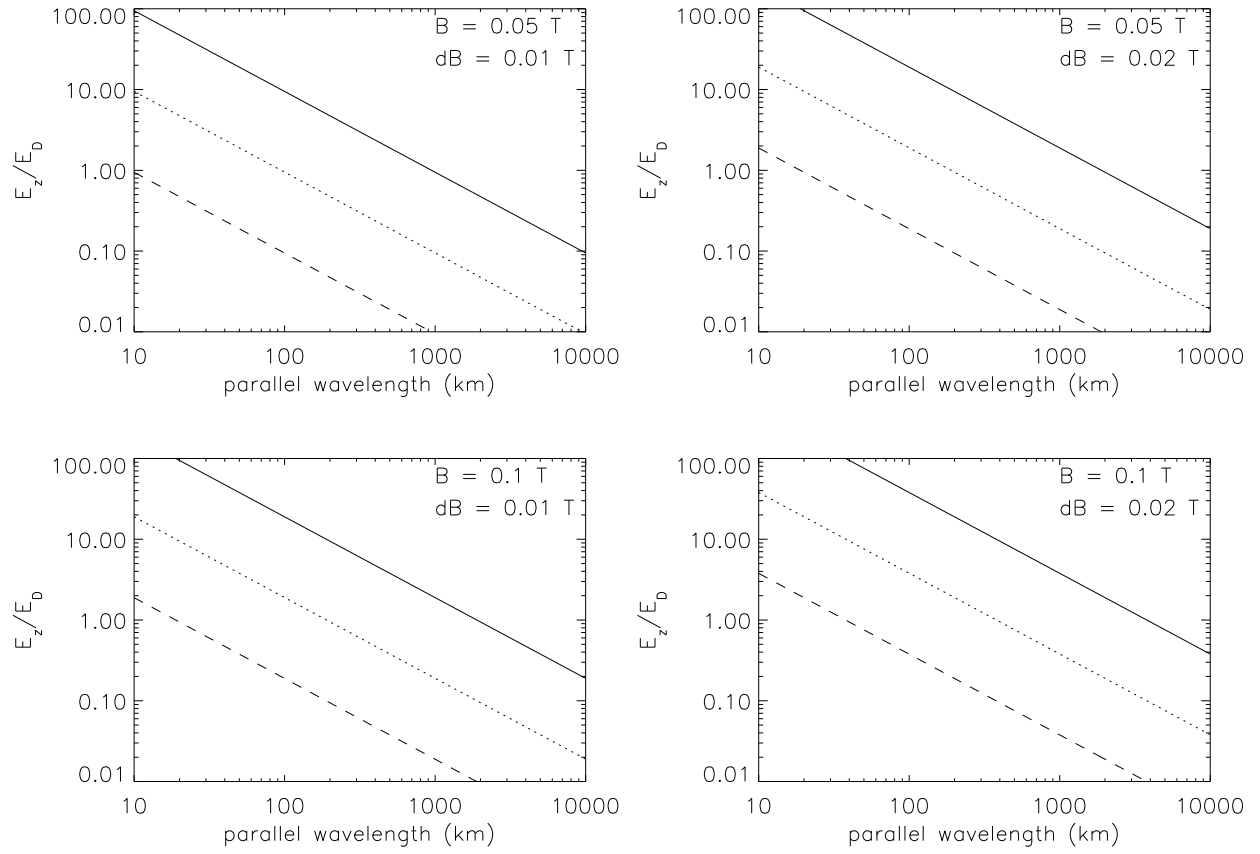


Fig. 5.— As in Figure 4, but with an electron density of $5 \times 10^{14} \text{m}^{-3}$.

traveling wave front, up to twice the Alfvén speed (Chaston 2006) thus gaining 4 times the ‘Alfvén energy’, $\frac{1}{2}m_e v_A^2$, corresponding to 27 keV for $B = 0.05$ T, and $n = 5 \times 10^{14} \text{m}^{-3}$. The maximum instantaneous electron flux from a single interaction of electrons with the wave field is $nv \sim 5 \times 10^{14} \text{m}^{-3} \times 2 \times 4.9 \times 10^7 \text{ms}^{-1} = 4.9 \times 10^{22} \text{m}^{-2} \text{s}^{-1}$ (this is comparable with typical electron fluxes inferred from hard X-rays of 10^{36}s^{-1} over an area of perhaps $10^{13} - 10^{14} \text{m}^2$). However, this flux will only be achieved if all electrons are accelerated, which will not happen because of the required velocity resonance condition of the electrons with the wavefront. Thus, waves with scales of tens to hundreds of kilometers may be capable of providing a modest flux of coronal electrons at 10 – 30 keV, running ahead of the wave front.

3.3. First-order Fermi acceleration in a moving mirror

Further acceleration can occur via a first-order Fermi process as the Alfvénic wave front, itself a moving mirror, approaches a magnetic mirror in the lower corona and chromosphere. In repeated reflections, the parallel electron speed would be increased by $2v_A$ at each interaction, until the resulting decrease of pitch angle allows the electron to penetrate the mirror. There is thus the possibility to accelerate a fraction of the injected electrons up to significantly higher energies.

For repeated reflections, the mirroring electrons must not be collisionally stopped between one interaction with the wavefront and the next. So the separation in column depth between wave-front and mirror must be less than half of the collisional stopping column depth of the electrons at $2v_A$ (neglecting the decreasing distance between wave-front and mirror as the pulse approaches the chromosphere). Using the expression from Emslie (1978), the collisional stopping column depth of an electron of energy E (in keV) is:

$$N_c = 10^{21} \mu_e E^2 \text{ m}^{-2}. \quad (9)$$

where μ_e is the electron pitch-angle cosine. So for an electron at 20 keV (i.e. following its first encounter with the wavefront), with a pitch angle of 45° , $N = \int n dl = 2.8 \times 10^{23} \text{m}^{-2}$. The electron must therefore mirror within $1.4 \times 10^{23} \text{m}^{-2}$. An underdense corona, of $n < 10^{15} \text{m}^{-3}$ with a loop half-length of 10^7 m, has $N < 10^{22} \text{m}^{-2}$, so a 20 keV electron could penetrate some way into the chromosphere - to a depth of around 1700 km above the photosphere in the VAL-C chromospheric model (a column mass of $2.3 \times 10^{-4} \text{kg m}^{-2}$). Thus, an electron could cross the corona and chromosphere, mirror quite deep down and return for further acceleration – producing bremsstrahlung emission en route. The details of this should be

worked out in future.

3.4. Turbulent Acceleration and Heating in the Chromosphere

We have seen that - with the possible exception of electron acceleration in their parallel electric field - Alfvén wave pulses will not dissipate significantly in the corona. This leads us to consider the consequences when the wave reaches the chromosphere, and to discuss ways in which the wave energy could be damped there. It is well known that, in a strongly-magnetized atmosphere, it is not easy to damp Alfvén waves by straightforward collisional means, either by ion-electron (Joule) or ion-ion (viscous) collisions (e.g. Osterbrock 1961). For this reason the dissipation of wave energy is normally thought to happen via a cascade process, with the energy ending up in wavelengths small enough for the Joule and viscous processes to be significant. (Note, ion-neutral damping probably is significant in the chromosphere and we return to this later). If such a cascade can develop, it will result in chromospheric heating, but possibly also electron acceleration. The theory of stochastic electron acceleration (e.g. Hamilton & Petrosian 1992; Larosa et al. 1994; Miller et al. 1996; Pryadko & Petrosian 1997; Petrosian & Liu 2004; Yan & Lazarian 2004; Petrosian et al. 2006) provides a possible mechanism for the acceleration of electrons into a broad spectrum extending to the high energies that are observed. There is an extensive literature on such acceleration processes; the reader is directed to Aschwanden (2002) (Section 5.2) for an overview of the process. Here we will mention only some aspects pertinent to the application of ideas of stochastic electron acceleration in this wave model within the collisional environment of the chromosphere. Firstly we discuss briefly the generation of the cascade itself.

As discussed in Section 2 it is reasonable to expect that some fraction of the Alfvén mode energy that arrives at the chromosphere will be reflected at the steep gradients within the chromosphere or from the photosphere, and allow the development of a turbulent spectrum in the counter-streaming wave field, with fast-mode and Alfvén components. To be viable, this should happen quickly - in less than the wave crossing-time of the chromosphere. There is a vast literature on the development of magnetic turbulence, but Yan & Lazarian (2004) provide useful expressions for the relevant timescales. The Alfvén spectrum develops within the turnover time of the longest wavelength present, λ_{max} , i.e. $t = \lambda_{max}/\delta v$ (see also Miller et al. 1996) where $\delta v/v_A = b_{\perp}/B$, δv being the velocity perturbation. So a (perpendicular) cascade with energy injected at wavelengths less than $\lambda = (b_{\perp}/B)$ times the height of the chromosphere can develop as the Alfvén waves cross the chromosphere. The development of the (isotropic) fast-mode spectrum, driven by reflected fast mode waves (Goedbloed & Halberstadt 1994) or fed by the Alfvén spectrum, depends on

the plasma β . In the high- β medium of the low chromosphere it develops in approximately $t = (\lambda_{max}/v_A)(v_A/\delta_V)^2$, so that only energy injected at relatively short wavelengths will cascade quickly enough. In the low- β upper chromosphere the development is yet slower.

Damping by Fermi acceleration will dominate in the chromosphere, compared to ion-viscous damping which may be significant in the corona. We demonstrate this by considering the ratio of the ion-viscous damping rate to the Fermi damping rate, given by (e.g. Tsap 2000):

$$\frac{\gamma_v}{\gamma_F} = \frac{\tau_F}{\tau_v} = 6 \times 10^{11} \frac{kT_i^{5/2}}{vn_a} \quad (10)$$

(converted into S.I. units) where k is the wavenumber, T_i the ion temperature, v the velocity, and n_a the density of particles accelerated by the Fermi mechanism. This ratio, plotted in Figure 6 for a range of different wavelengths of magnetoacoustic waves, is much less than one in the low temperature chromosphere, primarily because of the strong temperature dependence of the ion-viscous damping time. Therefore, chromosphere wavelengths longer than about 1 meter will be preferentially damped by Fermi acceleration (see also Petrosian et al. 2006) (however in the corona ion-viscous damping, though weak, can still be dominant).

Electron acceleration by a turbulent wave spectrum has been mostly studied in two main cases; ‘transit-time’ acceleration by low-frequency fast mode waves (e.g. Miller 1997; Lenters & Miller 1998; Yan & Lazarian 2002), and gyroresonant interaction with a whistler spectrum - the high frequency end of the Alfvén spectrum with $\omega > \Omega_i$ (e.g. Miller & Ramaty 1987; Hamilton & Petrosian 1992; Yan & Lazarian 2002; Petrosian & Liu 2004). Of particular importance to us is the effect in these models of Coulomb collisions: the dense chromosphere might be thought of as unfavorable for any particle acceleration to exist since energy gained can be quickly lost again. Some modeling has considered Coulomb energy losses and isotropization (e.g., Hamilton & Petrosian 1992; Lenters & Miller 1998; Yan & Lazarian 2004). In general, one finds that below the electron energy at which the acceleration timescale exceeds the collisional loss timescale, the electron distribution is quasi-thermal. Above this critical energy the distribution can have a non-thermal character as the electrons become increasingly collisionless at high energy. For whistler-mode acceleration, the critical energy is

$$E_c \sim 3.8n_{16}^{3/2} \left(\frac{0.01T}{|\mathbf{B}|} \right)^2 \left(\frac{10^{-4}}{R} \right) \text{keV} \quad (11)$$

where R is the ratio of turbulent magnetic energy density to total magnetic energy density (Hamilton & Petrosian 1992, Eq. 20). For chromospheric parameters of $n_{16} = 100$, $|\mathbf{B}| = 0.05$ then $E_c = 0.015/R$ keV. If the turbulent energy density fraction contained in whistlers is $R \sim 10^{-3}$ then the electron distribution will be non-thermal above 15 keV. It remains to be seen whether this level of whistler turbulence is plausible.

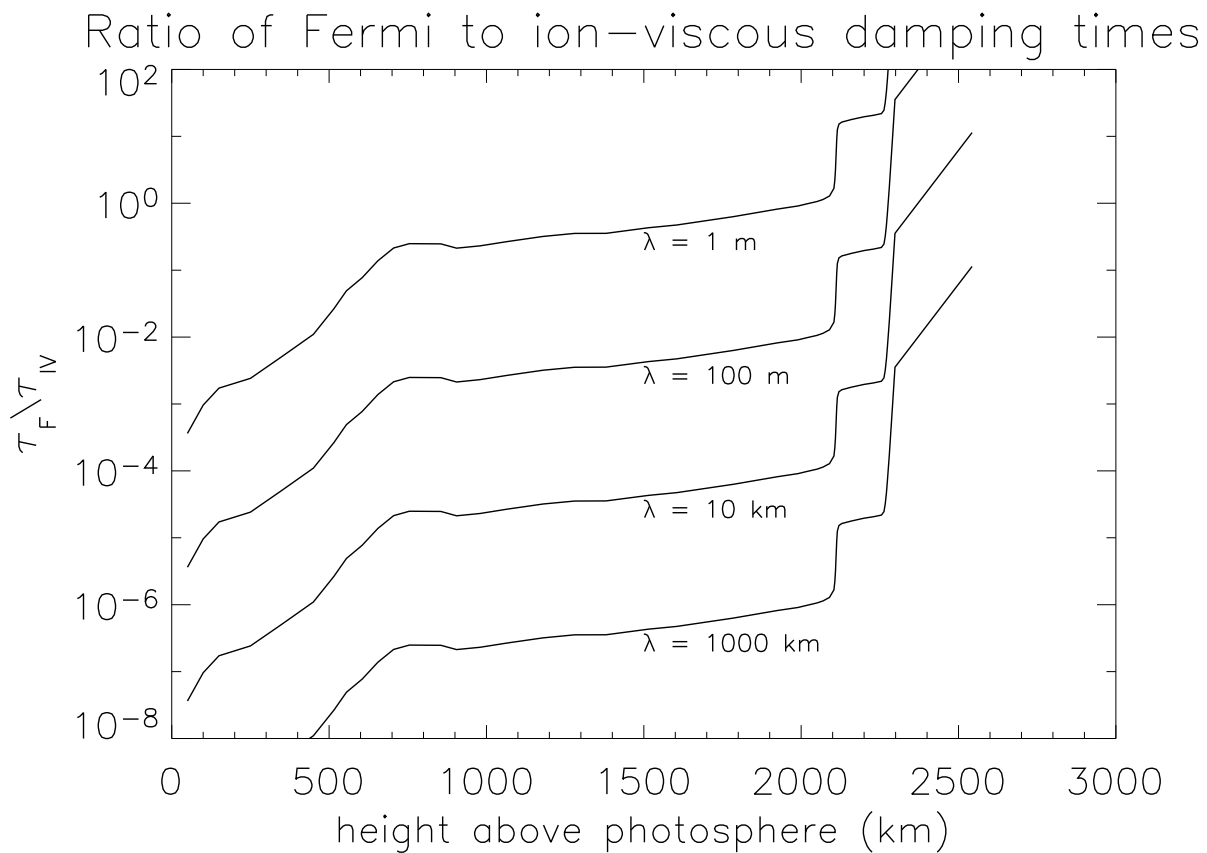


Fig. 6.— Ratio of the Fermi and ion-viscous damping times in the chromosphere, using a VAL-C model atmosphere. While this ratio may be much larger than unity in the corona, implying that ion-viscous damping dominates, it is less than unity throughout the chromosphere.

In the case of transit-time acceleration, which operates at much lower wave frequencies, Lenters & Miller (1998) find that energy exchange between waves and particles is in fact made significantly more efficient in the presence of Coulomb interactions. This is because Coulomb collisions (i) exchange energy between accelerated and non-accelerated electrons, raising the slower electrons up to resonant energies, and (ii) redistribute the energy gained between parallel and perpendicular components of momentum, increasing the magnetic moment of the electrons and thus the rate of the transit-time process. Transit-time damping by electrons requires that the local electron thermal speed be comparable to the Alfvén speed, equivalent to $\beta \sim m_e/m_p$. Using the VAL-C model, this occurs at around 1500 km above the photosphere, where the density is $\sim 10^{18} \text{ m}^{-3}$. It also requires that the wave spectrum be continuous (as in a turbulent spectrum), or at least have discrete overlapping modes to allow electrons to stay in resonance as they accelerate.

It should be noted that the simulations of Lenters & Miller (1998) are done for a temperature of $3 \times 10^6 \text{ K}$ and a density of 10^{16} m^{-2} . It remains to be seen whether the beneficial trade-off between energy loss and scattering will occur at higher densities, though since both scattering and loss terms in the Fokker-Planck equation describing the evolution of the particle distribution function have the same density dependence (see e.g. Lenters & Miller 1998 Eq. 4) we expect that it will.

However, even with the enhanced efficiency provided by Coulomb collisions, transit-time acceleration does not yield a power-law distribution as is observed from hard X-rays – instead it produces ‘bulk heating’ of electrons, albeit to energies of 10s of keV. Conceivably, a low level of whistler turbulence could provide the necessary pitch-angle scattering (but without energy redistribution) leading to the formation of an accelerated non-thermal tail.

4. Overall Energetics and Open Questions

We have introduced the idea of impulsive-phase transport of flare energy from its initial site of energy release via Alfvén wave pulses, and in the previous section have shown how this may lead to the electron acceleration needed to explain the hard X-ray observations. A complete theory should also address the generation of the wave energy in the first place, discuss the efficiency of the conversion, and describe the regulation mechanisms that allow the hard X-ray signatures to be so universal.

The partition of energy at its original source poses the first important question: what fraction goes into the Alfvén mode and what fraction goes into other wave modes? Emslie and Sturrock (1982) deal with this question qualitatively and suppose that half of the energy

winds up in the Alfvén mode and the other half in the fast mode, with the slow mode getting a negligible amount because of the mismatch between the sound speed and the Alfvén speed. To obtain a better understanding of this energy partition would require a full understanding of the non-linear development of the energy release, thus determining the flow fields involved in the deformation of the magnetic field. In a low- β plasma one would expect this deformation to proceed at or near the Alfvén speed.

The next step in the flow of energy consists of the Poynting flux S of the resulting waves, with $S \sim v_A \times b_{\perp}^2 / \mu_o$. The magnitude of the wave field b_{\perp} can be crudely estimated from the requirement that this Poynting flux supply the flare energy. Fletcher et al. (2007) show that the broadband flare output in moderate white-light and UV events, occurring in small footpoint areas, corresponds to an energy input in excess of $S \sim 10^7 \text{ J m}^{-2} \text{ s}^{-1}$. For an X-class flare energy dissipation of 10^{25} Joules in 10^3 seconds, over a spatial footpoint scale of $(10^4 \text{ km})^2$, we need $S \sim 10^8 \text{ J m}^{-2} \text{ s}^{-1}$. For $v_A \lesssim 1 \times 10^4 \text{ km s}^{-1}$ at the chromospheric formation depth of the broad-band emission, then $|b_{\perp}| \gtrsim 0.003 \text{ T}$. This is well within the upper limit to plausible field variations, given by the permanent line-of-sight field changes observed at the photosphere in large flares.

Other areas of theoretical uncertainty involve the degree of reflection of the wave energy on the gradients at and below the transition region, and the related question regarding the growth rate of the turbulent cascade. In the lower atmosphere the Alfvén speed varies over a scale short compared to the wavelength of the disturbance, so the disturbance will be partially reflected and partially transmitted (though the fact that stepwise photospheric field changes of order ten percent are seen suggests that a considerable fraction of wave energy is transmitted to the photospheric level). Emslie & Sturrock (1982) discuss wave transport and dissipation in the context of a normal solar atmospheric model, in which thermal conduction creates a sharp transition layer. In this case substantial wave reflection will occur, launching a propagating wave towards the conjugate footpoint. The coefficient of reflection is given by $R_E = (\theta^{1/2} - 1)^2 / (\theta^{1/2} + 1)^2$ where θ represents the temperature ratio between corona and chromosphere. For a quiet solar atmosphere we might have $\theta = 200$ and $R_E \sim 75\%$, but clearly in a flaring atmosphere this estimate will have to be modified and will affect the wave energy reaching the chromosphere. Strong heating should increase the scale height, soften the transition region and reduce the reflected component. In the radiative hydrodynamic models of Allred et al. (2005), the density and temperature gradients between chromosphere and corona are indeed at first on average smoothed out by atmospheric heating in the impulsive phase, but then steeper temperature gradients occur as the corona heats. But the behavior also varies with the intensity, and location of heat input, which depends of course on the energy transport model and atmospheric structure, and will need to be examined in detail.

The energy of the transmitted fraction will be dissipated in the chromosphere. Alfvénic disturbances can damp resistively, if on small enough scales, or by other means such as ion-neutral coupling which may be particularly important in the lower chromosphere. De Pontieu et al. (2001) considered the damping by ion-neutral coupling in the lower chromosphere of large-scale coronal oscillations, observed in TRACE to be excited by flares and filament eruptions (Schrijver et al. 2002). Although these waves are kink (fast mode) waves in flux tubes with relatively low fields, analogous damping may occur for our Alfvén mode waves in strong field regions. The Joule dissipation as calculated by Emslie & Sturrock is enhanced by a factor $(1 + s)$ where s is the “ion slip” term;

$$s = \left(\frac{\rho_n}{\rho_t} \right)^2 \frac{\Omega_e \Omega_i}{\nu_{eff} \nu_{in}}; \quad (12)$$

here Ω_e and Ω_i are the electron and ion gyrofrequencies, $\nu_{eff} = \nu_{ei} + \nu_{en}$, the collision frequencies of electrons on ions and neutrals, respectively, and ν_{in} is the ion-neutral collision frequency. De Pontieu et al. found the slip s to be large throughout the chromosphere, resulting in Joule heating that peaks between around 300 km and 1000 km above the photosphere. This is close to the temperature minimum region where localized energy input is required to generate the observed white-light flare continuum excess.

Finally, any remaining undamped waves, once reflected at the photosphere or at strong chromospheric gradients may lead to the development of a turbulent cascade which, as we have noted, provides one of the major possibilities for chromospheric electron acceleration. Again a quantitative description of this partitioning is beyond the scope of this paper.

5. Conclusions

Energy transport by Alfvén waves has a well-developed literature in the context of the terrestrial aurora, and we have applied similar ideas here to the problem of flare effects in the solar atmosphere. Our new understanding of active-region magnetic fields, based on microwave observations, now convinces us that the transport time for these waves is very short – short enough to explain the rapid time variations and tight conjugacy of double-footpoint hard X-ray sources – and also that the energy flux can be very large. From this point of view, Alfvén waves therefore provide an alternative to energy transport by electron beams. Emslie & Sturrock aimed at explaining a relatively weak warming of the temperature-minimum region late in the flare, as required by Ca K line observations of Machado et al. (1978). We instead wish to explain the entire energy of the flare impulsive phase in this manner.

Replacing the electron beam of the standard thick-target model with an Alfvén-wave Poynting flux implies particle acceleration in the chromosphere or at the base of the coronal loop carrying the wave. Because of the dominance of fast electrons in the flare energy budget, we have discussed mechanisms for electron acceleration in this scenario at length. Our analysis establishes the feasibility of these ideas without pinpointing which of the possible acceleration modes dominates.

Finally, we note that the ideas we present are novel in the solar context but are well-established in the Earth’s magnetosphere. These ideas should be considered not only for solar flares, but elsewhere in the Universe where magnetic reconnection is invoked.

We would like to acknowledge many useful discussions with numerous colleagues, including J. C. Brown, P. Cargill, C. Chaston, P. Damiano, N. Gopalswamy, G. Haerendel, J. I. Khan, E. P. Kontar, A. L. MacKinnon, J. P. McFadden and K. Shibata. We would also like to thank an anonymous referee for vigorous discussion which led to significant improvements in the overall structure and clarity of the paper. This work was supported by NASA under grants NNG05GG17G (L. F. and H. S. H) and NAS 5-98033 (H. S. H.), and by PPARC under Rolling Grant PP/C000234/1 (L.F.). Financial support by the European Commission through the SOLAIRE Network (MTRN-CT-2006-035484) is gratefully acknowledged.

REFERENCES

- Allred, J. C., Hawley, S. L., Abbett, W. P., & Carlsson, M. 2005, *ApJ*, 630, 573
- Aschwanden, M. J. 2002, *Space Science Reviews*, 101, 1
- Battaglia, M. & Benz, A. O. 2006, *A&A*, 456, 751
- Berger, T. E., Rouppe van der Voort, L. H. M., Löfdahl, M. G., Carlsson, M., Fossum, A., Hansteen, V. H., Marthinussen, E., Title, A., & Scharmer, G. 2004, *A&A*, 428, 613
- Bogachev, S. A., Somov, B. V., Kosugi, T., & Sakao, T. 2005, *ApJ*, 630, 561
- Brosius, J. W., Landi, E., Cook, J. W., Newmark, J. S., Gopalswamy, N., & Lara, A. 2002, *ApJ*, 574, 453
- Brosius, J. W. & White, S. M. 2006, *ApJ*, 641, L69
- Brown, J. C. 1971, *Sol. Phys.*, 18, 489
- . 1973, *Sol. Phys.*, 28, 151

- Cameron, R. & Sammis, I. 1999, *ApJ*, 525, L61
- Chaston, C. C. 2006, American Geophysical Union Geophysical Monograph Series, 166, 239
- Chaston, C. C., Bonnell, J. W., Peticolas, L. M., Carlson, C. W., McFadden, J. P., & Ergun, R. E. 2002, *Geophys. Res. Lett.*, 29, 30
- Cranmer, S. R. & van Ballegoijen, A. A. 2005, *ApJS*, 156, 265
- Damiano, P. A. & Wright, A. N. 2005, *Journal of Geophysical Research (Space Physics)*, 110, 1201
- De Pontieu, B., Martens, P. C. H., & Hudson, H. S. 2001, *ApJ*, 558, 859
- Del Zanna, G. & Mason, H. E. 2003, *A&A*, 406, 1089
- Dennis, B. R. 1985, *Sol. Phys.*, 100, 465
- Doschek, G. A., Strong, K. T., & Tsuneta, S. 1995, *ApJ*, 440, 370
- Dreicer, H. 1959, *Physical Review*, 115, 238
- Emslie, A. G. 1978, *ApJ*, 224, 241
- Emslie, A. G. & Sturrock, P. A. 1982, *Sol. Phys.*, 80, 99
- Fárník, F., Hudson, H., & Watanabe, T. 1996, *Sol. Phys.*, 165, 169
- Fárník, F. & Savy, S. K. 1998, *Sol. Phys.*, 183, 339
- Fletcher, L. & De Pontieu, B. 1999, *ApJ*, 520, L135
- Fletcher, L., Hannah, I. G., Hudson, H. S., & Metcalf, T. R. 2007, *ApJ*, 656, 1187
- Forbes, T. G. & Acton, L. W. 1996, *ApJ*, 459, 330
- Goedbloed, J. P. & Halberstadt, G. 1994, *A&A*, 286, 275
- Goertz, C. K. & Boswell, R. W. 1979, *J. Geophys. Res.*, 84, 7239
- Gosling, J. T., Skoug, R. M., McComas, D. J., & Smith, C. W. 2005, *Journal of Geophysical Research (Space Physics)*, 110, 1107
- Hamilton, R. J. & Petrosian, V. 1992, *ApJ*, 398, 350
- Heyvaerts, J. & Priest, E. R. 1983, *A&A*, 117, 220

- Holman, G. D., Sui, L., Schwartz, R. A., & Emslie, A. G. 2003, *ApJ*, 595, L97
- Hudson, H. S. 1972, *Sol. Phys.*, 24, 414
- Kane, S. R. & Donnelly, R. F. 1971, *ApJ*, 164, 151
- Kinney, R. M. & McWilliams, J. C. 1998, *Phys. Rev. E*, 57, 7111
- Kletzing, C. A. 1994, *J. Geophys. Res.*, 99, 11095
- Kosovichev, A. G. & Zharkova, V. V. 2001, *ApJ*, 550, L105
- Landi, E., Feldman, U., Innes, D. E., & Curdt, W. 2003, *ApJ*, 582, 506
- Larosa, T. N., Moore, R. L., & Shore, S. N. 1994, *ApJ*, 425, 856
- Lee, J., McClymont, A. N., Mikic, Z., White, S. M., & Kundu, M. R. 1998, *ApJ*, 501, 853
- Lenters, G. T. & Miller, J. A. 1998, *ApJ*, 493, 451
- Lin, R. P. & Hudson, H. S. 1976, *Sol. Phys.*, 50, 153
- Linton, M. G. & Longcope, D. W. 2006, *ApJ*, 642, 1177
- Litvinenko, Y. E. 2003, in *Lecture Notes in Physics*, Berlin Springer Verlag, Vol. 612, *Energy Conversion and Particle Acceleration in the Solar Corona*, ed. L. Klein, 213–229
- MacKinnon, A. L. 2006, *American Geophysical Union Geophysical Monograph Series*, 165, 157
- Melrose, D. B. 1992, *ApJ*, 387, 403
- Miller, J. A. 1997, *ApJ*, 491, 939
- Miller, J. A., Larosa, T. N., & Moore, R. L. 1996, *ApJ*, 461, 445
- Miller, J. A. & Ramaty, R. 1987, *Sol. Phys.*, 113, 195
- Nakariakov, V. M. & Ofman, L. 2001, *A&A*, 372, L53
- Osterbrock, D. E. 1961, *ApJ*, 134, 347
- Petrosian, V. & Liu, S. 2004, *ApJ*, 610, 550
- Petrosian, V., Yan, H., & Lazarian, A. 2006, *ApJ*, 644, 603
- Pryadko, J. M. & Petrosian, V. 1997, *ApJ*, 482, 774

- Roberts, B. 2000, *Sol. Phys.*, 193, 139
- Sakao, T. 1994, PhD thesis, (University of Tokyo), (1994)
- Schrijver, C. J., Aschwanden, M. J., & Title, A. M. 2002, *Sol. Phys.*, 206, 69
- Shibasaki, K., Enome, S., Nakajima, H., Nishio, M., Takano, T., Hanaoka, Y., Torii, C., Sekiguchi, H., Kawashima, S., Bushimata, T., Shinohara, N., Koshiishi, H., Shiomi, Y., Irimajiri, Y., Leka, K. D., & Canfield, R. C. 1994, *PASJ*, 46, L17
- Smith, D. F. & Lilliequist, C. G. 1979, *ApJ*, 232, 582
- Solanki, S. K. 2003, *A&A Rev.*, 11, 153
- Spicer, D. S. 1982, *Space Science Reviews*, 31, 351
- Stasiewicz, K. 2006, *Physical Review Letters*, 96, 175003
- Stasiewicz, K., Bellan, P., Chaston, C., Kletzing, C., Lysak, R., Maggs, J., Pokhotelov, O., Seyler, C., Shukla, P., Stenflo, L., Streltsov, A., & Wahlund, J.-E. 2000, *Space Science Reviews*, 92, 423
- Stasiewicz, K., Nordblad, E., & Lindstedt, T. 2007, *Physical Review Letters*, 98, 049502
- Sudol, J. J. & Harvey, J. W. 2005, *ApJ*, 635, 647
- Tsap, Y. T. 2000, *Sol. Phys.*, 194, 131
- Tsiklauri, D. 2006, *A&A*, 455, 1073
- Varady, M., Fludra, A., & Heinzl, P. 2000, *A&A*, 355, 769
- Vernazza, J. E., Avrett, E. H., & Loeser, R. 1981, *ApJS*, 45, 635
- Veronig, A. M. & Brown, J. C. 2004, *ApJ*, 603, L117
- Vourlidas, A., Gary, D. E., & Shibasaki, K. 2006, *PASJ*, 58, 11
- Watt, C. E. J. & Rankin, R. 2007, *Journal of Geophysical Research (Space Physics)*, 112, 4214
- Watt, C. E. J., Rankin, R., & Marchand, R. 2004, *Physics of Plasmas*, 11, 1277
- Wheatland, M. S. & Melrose, D. B. 1994, *Proceedings of the Astronomical Society of Australia*, 11, 25

- White, S. M., Kundu, M. R., & Gopalswamy, N. 1991, *ApJ*, 366, L43
- Wright, A. N., Allan, W., & Damiano, P. A. 2003, *Geophys. Res. Lett.*, 30, 2
- Wright, A. N., Allan, W., Ruderman, M. S., & Elphic, R. C. 2002, *Journal of Geophysical Research (Space Physics)*, 107, 19
- Wright, A. N. & Hood, A. W. 2003, *Journal of Geophysical Research (Space Physics)*, 108, 22
- Wygant, J. R., Keiling, A., Cattell, C. A., Lysak, R. L., Temerin, M., Mozer, F. S., Kletzing, C. A., Scudder, J. D., Streltsov, V., Lotko, W., & Russell, C. T. 2002, *Journal of Geophysical Research (Space Physics)*, 107, 24
- Yan, H. & Lazarian, A. 2002, *Physical Review Letters*, 89, B1102+
- . 2004, *ApJ*, 614, 757
- Zweibel, E. G. & Haber, D. A. 1983, *ApJ*, 264, 648